

Automatic computation of pebble roundness using digital imagery and discrete geometry

Tristan Roussillon ^a, Hervé Piégay ^b, Isabelle Sivignon ^c,

Laure Tougne ^a, Franck Lavigne ^d

^a*University of Lyon, LIRIS, 5 Av Pierre-Mendès France 69676 Bron*

^b*University of Lyon, CNRS-UMR 5600 Environnement, Ville, Société, 15 Parvis René
Descartes, 69364 Lyon*

^c*University of Lyon, LIRIS, CNRS, 8 Bd Niels Bohr 69622 Villeurbanne*

^d*University of Paris, CNRS-UMR 8591 Laboratoire de Géographie Physique, 1 place
Aristide Briand, 92195 Meudon*

Abstract

The shape of sedimentary particles is an important property, from which geographical hypotheses related to abrasion, distance of transport, river behavior, etc. can be formulated. In this paper, we use digital image analysis, especially discrete geometry, to automatically compute some shape parameters such as roundness i.e. a measure of how much the corners and edges of a particle have been worn away.

In contrast to previous works in which traditional digital images analysis techniques such as Fourier transform (Diepenbroek et al., 1992, *Sedimentology*, 39) are used, we opted for a discrete geometry approach that allowed us to implement Wadell's original index (Wadell, 1932, *Journal of Geology*, 40) which is known to be more accurate, but more time consuming to implement in the field (Pissart et al., 1998, *Géomorphologie: relief, processus, environnement*, 3).

Our implementation of Wadell's original index is highly correlated (92%) with the roundness classes of Krumbein's chart, used as a ground-truth (Krumbein, 1941, *Journal of Sedimentary Petrology*, 11, 2). In addition, we show that other geometrical parameters, which are easier to compute, can be used to provide good approximations of roundness.

We also used our shape parameters to study a set of pebbles digital images taken from the Progo basin river network (Indonesia). The results we obtained are in agreement with previous works and open new possibilities for geomorphologists thanks to automatic computation.

Key words: Sedimentary particle, Shape description, Discrete geometry, Roundness, Physical abrasion, Bedload transport, River continuum

1 Introduction

The shape of sedimentary particles is an important property from which geographical hypotheses related to abrasion, distance of transport, river behavior, etc. can be formulated (e.g. Krumbein, 1941). The main shape features are form or sphericity (a sphere similarity measure), roundness (a measure of how much the corners and edges of a pebble have been worn away) and surface texture (a measure of small-scale features) (Diepenbroek et al., 1992).

Roundness of a particle was initially defined by Wadell (1932). This method of estimating roundness is infrequently used even though it is known to be more accurate than other methods (Pissart et al., 1998), because the required number of measurements is time consuming. For each particle, the radius of curvature of each corner has to be measured either on three orthogonal planes or on the silhouette. A corner is defined as a part of the contour for which the radius of curvature is lower than the radius of the largest inscribed circle. The ratio between the mean

15 radius of curvature of the corners and the radius of the largest inscribed circle de-
16 fines the roundness measure (Wadell, 1932) (figure 1). No definition of curvature
17 was given in the original paper. In order to shorten the time required to estimate
18 roundness, Krumbein (1941) created a chart (figure 2). Krumbein's chart shows
19 examples of pebbles for which the roundness of their silhouette has been calcu-
20 lated using Wadell's method and clusters them into 9 classes. Some field guidelines
21 (Bunte and Abt, 2001) recommend a visual estimate of pebble roundness based on
22 the chart. In order to shorten the measurement time while keeping a certain objec-
23 tivity, some authors have proposed indices that were inspired by Wadell's index, but
24 easier to calculate (e.g. Cailleux, 1947). Pissart et al. (1998) found that the Cailleux
25 and Krumbein methods give similar results on average, with the Krumbein method
26 being much quicker.

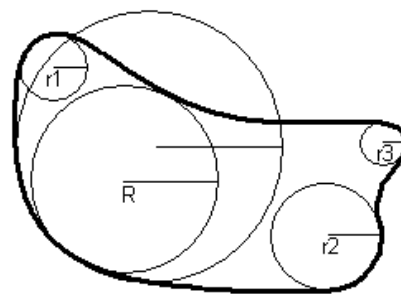


Fig. 1. Roundness definition (Wadell, 1932). On the one hand, the radius r_1 , r_2 et r_3 , being smaller than the radius R of the largest inscribed circle, define and measure corners. On the other hand, the circle without label, being greater than the radius R of the largest inscribed circle, does not define nor measure a corner. As a consequence, roundness is the average of r_1 , r_2 , r_3 .

27 Our objective is to reduce the subjectivity and time measurement required for the
28 estimation of pebble roundness by providing an automatic computation method
29 for Wadell's index. Although several methods have been proposed that provide an
30 estimate that is linearly correlated with the values given by the Krumbein's chart,

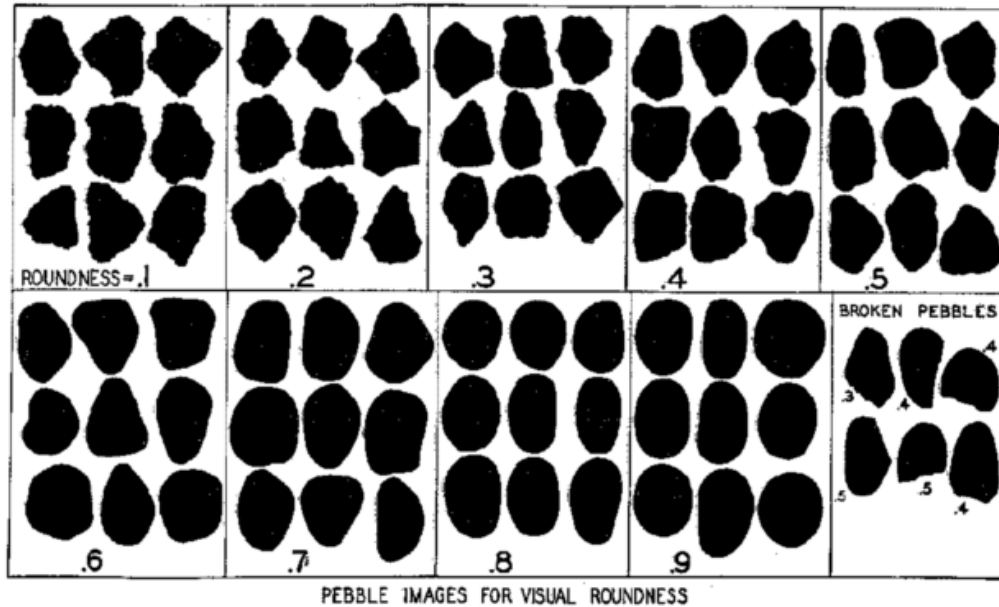


Fig. 2. Krumbein's chart (Krumbein, 1941).

31 a method that automatically calculates Wadell's original index has not yet been
 32 developed.

33 One of the roundness determination methods is based on the Fourier transform. A
 34 well-known method has been proposed by Diepenbroek et al. (1992). This method
 35 takes as input the polar coordinates of a sample of 64 points of the particle bound-
 36 ary, spaced at equal angular intervals. The Fourier transform is computed from the
 37 distance to the centroid. The weighted sum of the amplitudes of the first 24 coeffi-
 38 cients of the Fourier transform is a roundness estimate. To remove size information,
 39 the coefficients are divided by the zeroth coefficient. In addition, sphericity aspect
 40 is eliminated by subtracting the spectrum of the best approximating ellipse from
 41 that spectrum. The measure obtained was found to be linearly correlated (94%)
 42 with the values of Krumbein's chart.

43 An alternative method using mathematical morphology was proposed by Drevin
 44 and Vincent (2002). The idea is to apply a morphological opening on a particle

45 silhouette. The morphological opening consists of an erosion and a dilation with a
46 same structuring element, so that some shape features like 'cape' or 'isthmus' are
47 removed without a contraction of the silhouette. The ratio between the particle area
48 before and after the morphological opening is a roundness measure again linearly
49 correlated (96%) with the values of Krumbein's chart, with a circular structuring
50 element of radius equal to 42% of the radius of the largest inscribed circle.

51 The aim of this paper is to develop a method to automatically calculate the Wadell's
52 pioneering roundness index, as well as the index of Drevin and Vincent (2002). We
53 will also develop new indices based on particule geometry to study roundness with
54 respect to form and size, notably the ratio between perimeters of the silhouette and
55 of the best approximating ellipse, which has been positively correlated to the val-
56 ues of the Krumbein's chart. As we choose to focus on geometrical parameters, we
57 do not implement parameters that use signal processing like the index proposed by
58 Diepenbroek et al. (1992). This work should help to accelerate the sediment sam-
59 pling process in river studies and allow the development of geographical hypotheses
60 related to sediment particle roundness at the river network scale.

61 The paper is organised as follows. In section 2, we describe the shape parameters
62 we implemented and give some details about the implementation of the Wadell's
63 index. In section 3, we compare different shape parameters using Krumbein's chart.
64 Experiments are described in section 4 with real images. Conclusions and future
65 research directions are presented in section 5.

66 2 Computation of shape parameters using discrete geometry

67 In this section we consider a binary image of a pebble. The image has been taken
68 such that it coincides with the maximum projection plane of the pebble (this is what
69 we called the *silhouette* of the particle in figure 3). From this silhouette we compute
70 one size parameter and some form and roundness parameters.

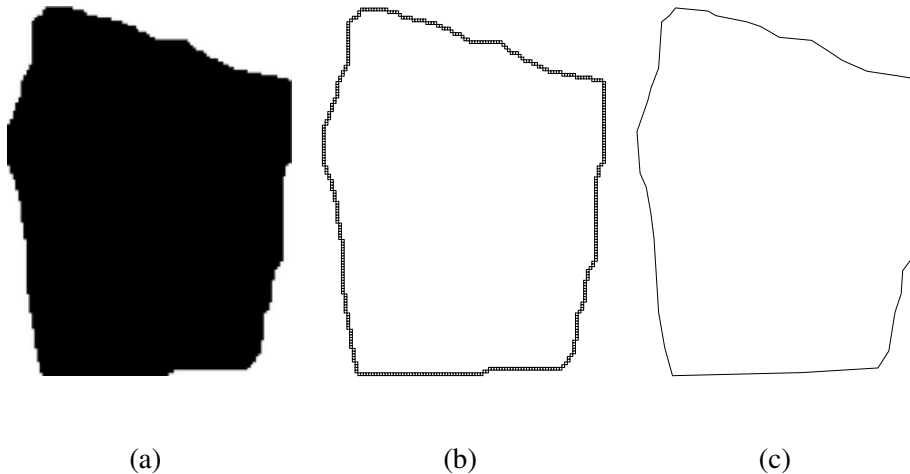


Fig. 3. A silhouette of a particle in (a) and its boundary in (b). The polygonalisation of the boundary is in (c).

71 2.1 Size parameter

72 Traditionally, the most frequently used size parameters are the lengths of the three
73 representative axes: a (major axis), b (medium axis), c (minor axis). Using the ro-
74 tating calipers algorithm (Toussaint, 1983), a basic tool of computational geometry
75 (Preparata and Shamos, 1985), we can easily estimate a and b from the silhouette
76 of a particle. The idea is to rotate two parallel lines around the silhouette, such that
77 the silhouette is enclosed by the two lines and the two lines touch the silhouette:
78 a is the maximum distance between such parallel lines and b is the minimum dis-
79 tance between such parallel lines. We take b as a measure of the particle size, the

80 so-called b-axis of the particles (Bunte and Abt, 2001).

81 2.2 Form parameters

82 **Circularity**, defined as the ratio between the perimeters of the silhouette and of a
83 disk of same area as the silhouette, is a basic descriptor in digital image analysis.
84 It can be seen as a two-dimensional equivalent of sphericity. If P_S and A_S denote
85 respectively the perimeter and the area of the silhouette, the formula is:

$$circularity = \frac{P_S}{2\sqrt{A_S\pi}} \quad (1)$$

86 Before computing the perimeter and area of the silhouette, we extracted the bound-
87 ary of the silhouette by contour tracking and we polygonalised the sequence of
88 8-connected pixels with a digital straight segment recognition algorithm (Debled-
89 Rennesson and Reveilles, 1995) (figure 3). Next, area and perimeter were computed
90 from the obtained polygon.

91 From a theoretical point of view, we used the arithmetical definition of the digital
92 straight line, which leads to an algorithm that is linear in time with integer-only
93 computations. In addition, it is proven that if the image resolution is infinitely high,
94 then the perimeter and area estimations are infinitely close to the true values (Klette
95 and Zunic, 2000).

96 However *circularity* is difficult to interpret because it confounds size, elongation,
97 convexity and roundness information. We propose to study these parameters inde-
98 pendently and their definitions are given hereafter:

99 **Elongation** is easy to compute and is equal to the ratio between b and a .

$$elongation = \frac{b}{a} \quad (2)$$

100 **Convexity** is defined as the ratio between the area of the silhouette (A_S) and of
 101 the convex hull of the silhouette (A_{CH}). A convex hull is defined as the minimal
 102 convex polygon covering of an object. The convex hull has been thoroughly studied
 103 in computational geometry (Preparata and Shamos, 1985) and is computed here
 104 with the algorithm of Melkman (1987).

$$convexity = \frac{A_S}{A_{CH}} \quad (3)$$

105 2.3 Roundness parameters

106 Wadell defined his roundness index as follow:

$$rW = \frac{1}{k \cdot R} \sum_{i=1}^k r_i \quad (4)$$

107 where r_i is the radius of curvature that is smaller than or equal to the radius of
 108 curvature R of the largest inscribed disk at a pixel on the boundary of the pebble
 109 silhouette and k is the number of such radii.

110 The implementation of rW followed three steps:

111 (1) The radius of curvature at each pixel was estimated in a robust way using an
 112 algorithm illustrated in figure 4 (Nguyen and Debled-Rennesson, 2007).

113 First, the longest sequences of 8-connected pixels lying between two paral-
 114 lel straight lines separated by a given distance d to the left and to the right of
 115 P were identified. In figure 4 and hereafter $d = 2$. The end of the sequence of

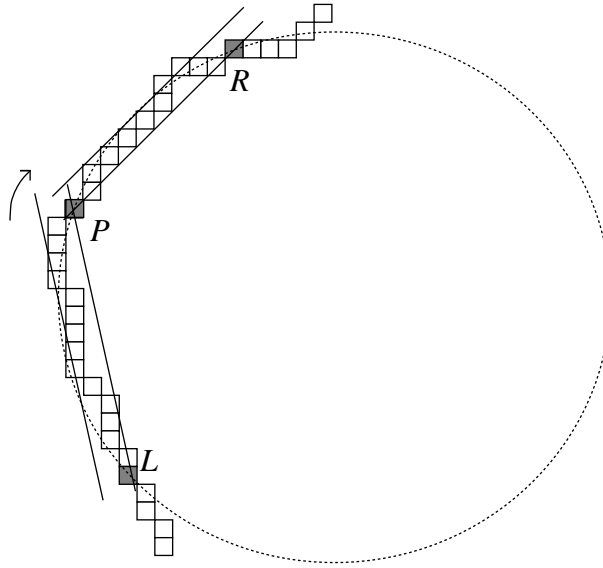


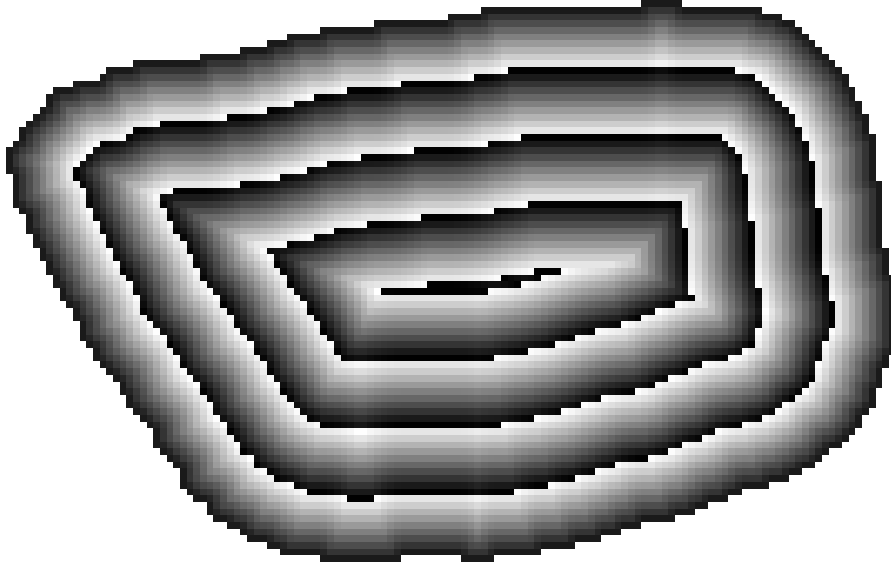
Fig. 4. An example of the computation of the radius of curvature at a pixel P . The radius of curvature is the radius of the circle (dotted line) passing through LPR .

116 8-connected pixels to the left (resp. to the right) of P is denoted by L (resp.
 117 R). Next, the radius of the circumcircle of the triangle LPR was computed.
 118 This procedure was repeated for each pixel.

119 (2) The radius of the largest inscribed disk is calculated using the distance trans-
 120 form of the silhouette. The distance transform is a frequently-used tool in
 121 discrete geometry that consists of labelling each pixel of the silhouette by its
 122 distance to the nearest pixel not belonging to the silhouette (figure 5). It was
 123 computed using the efficient algorithm of Hirata (1996).

124 (3) rW was calculated using equation 4. Only the pixels with a radius of curvature
 125 smaller or equal than the radius of curvature of the largest inscribed disk were
 126 taken into account (figure 6).

127 For comparison, we also calculated the roundness measure proposed by Drevin and
 128 Vincent (2002). This parameter is also geometrical because the basic morphological
 129 operations are related to the distance transform, the tool used to compute the radius
 130 of the largest inscribed disk.



50

Fig. 5. Distance transform of a pebble silhouette. Each pixel is filled with a grey level according to its distance to the nearest pixel not belonging to the silhouette (modulo 10). The radius of the largest inscribed circle is 40.6.

$$rD = \frac{A_{S \oplus C(o,r_c) \ominus C(o,r_c)}}{A_S} \quad (5)$$

131 where $A_{S \oplus C(o,r_c) \ominus C(o,r_c)}$ denotes the area of the silhouette after a morphological
 132 opening with a circular structuring element C of center o and radius r_c . As in
 133 equations 1 and 3, A_S denotes the area of the silhouette. Operators \oplus and \ominus de-
 134 note Minkowski's addition (dilatation or thresholding in the distance transform of
 135 the complementary set of the silhouette) and Minkowski's subtraction (erosion or
 136 thresholding in the distance transform of the silhouette) respectively. The radius r_c
 137 of the circular structuring element was fixed to 75% of the radius R of the largest
 138 inscribed disk. This is the percentage for which rD had the best correlation with
 139 the values of Krumbein's chart (section 3).

140 As stated above, we chose to focus on geometrical parameters and therefore we



Fig. 6. The radius of curvature is computed for each pixel. The darker the pixel, the smaller the radius of the curvature. Only pixels whose radius of curvature is less than the radius of the largest inscribed circle, are taken into account in the roundness calculation. The roundness is the ratio between the average of the radius of curvature of retained pixels (28.5) and the radius of the largest inscribed circle (40.6), that is 0.70.

141 do not implement parameters based on signal processing like the one proposed by
 142 (Diepenbroek et al., 1992).

143 Finally, because it has been previously correlated to the Wadell's index (Cottet,
 144 2006), we also computed the ratio between the perimeter of the silhouette (P_S) and
 145 of the best approximating ellipse (P_e) as a last roundness measure as follows:

$$rP = \frac{P_S}{P_e} \quad (6)$$

146 Since *circularity*, which consists in comparing the silhouette with a circle, in-
 147 cludes both size, elongation and roundness information, the idea is to compare the
 148 silhouette with an ellipse, instead of a circle, to remove size and elongation aspects

149 and capture only the roundness.

150 2.4 Behavior of shape parameters with respect to resolution

151 In this section, the behavior of our shape parameters is studied with respect to
152 resolution. We used synthetic images, so that the resolution was controlled and the
153 true values of our shape parameters were known.

154 We assumed an orthogonal grid with a uniform spacing denoted by l between the
155 grid points. We assumed that in a digital image, pixels are grid points. The res-
156 olution of the image r is defined as $r = 1/l$. Geometrical shapes were digitized
157 such that pixels located inside and outside the shape were labelled *object* and *back-*
158 *ground* respectively. To increase the resolution r , we may shrink the grid as well as
159 leave the grid fixed and dilate the shape (Klette and Zunic, 2000). Therefore, the
160 shape parameters introduced above were computed on digitized ellipses of increas-
161 ing size (figure 7). An ellipse was used instead of a polygon (or a circle that is a
162 specific case of the ellipse), because most of parameters, which are based on digital
163 straight segment recognition (*circularity*, *convexity*, rP , rW), are more accurate
164 when the geometrical shape is a polygon and an ellipse thus allowed us to test the
165 worst-case scenario.

166 The curves of three of the five parameters (*convexity*, *circularity*, rP) are really
167 smooth and converge very quickly towards the true values (1, approximately 0.83
168 and 1 respectively). These parameters are computed thanks to very accurate perime-
169 ter and area estimators. The curves of the two others (rD and rW) are less smooth
170 and converge more slowly to constant values as the size of the digitized ellipses in-
171 creases. The true values of rD and rW are difficult to compute. However, a coarse

Form and roundness of digital ellipses of increasing size

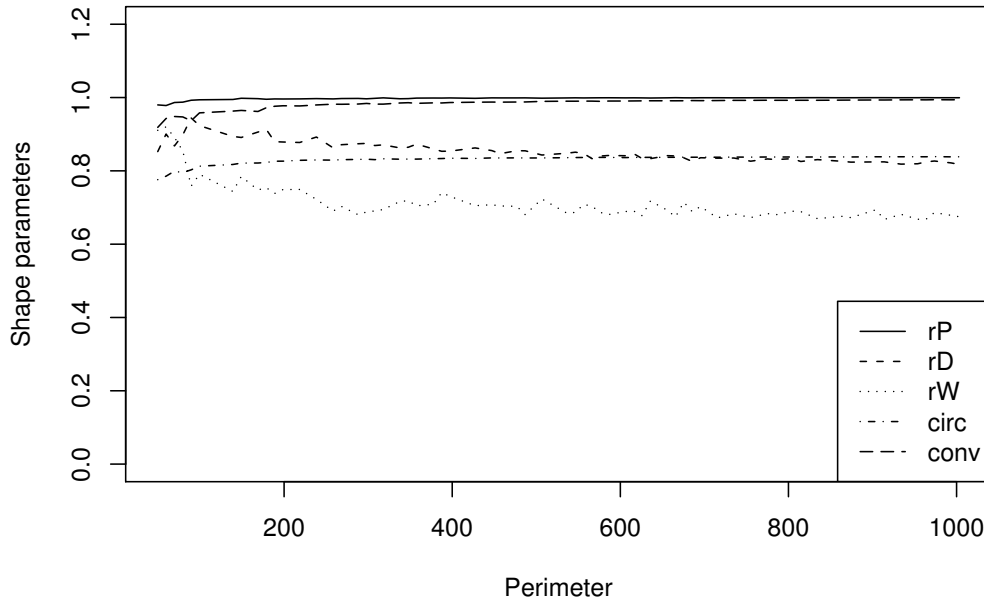


Fig. 7. Shape parameters introduced in section 2 (*circ*: circularity, *conv*: convexity, *rD*: Drevin’s roundness, *rW*: Wadell’s roundness, *rP*: ratio between perimeters of the silhouette and of the best approximating ellipse) over perimeter of digital ellipses. A digital ellipse is the set of pixels the center of which is located inside a euclidean ellipse. The elongation of the digital ellipses is fixed and equals $1/2$, whereas the perimeter ranges from 10 to 1000.

172 estimation of ground truth (e.g. around 0.6 or 0.65 for *rW*) as well as the accuracy
173 of the tools used for the computation (an exact euclidean distance transform and
174 a robust curvature estimation for *rW*) allow confidence that the computed values
175 approach the true values.

176 The above analysis suggests that to remove the influence of the resolution, a silhouette
177 minimum size has to be used. To do so, a threshold on the shape perimeter is
178 set: beyond this threshold, the error is considered acceptable. In figure 7, the error
179 is less than 10% for all shape parameters above a perimeter of 150 pixels. We con-
180 clude that measures are accurate for all shape parameters, if the perimeter of the

181 extracted boundary of each pebble is above this value.

182 3 Correlations study using Krumbein's chart

183 In table 1, the correlation between the individual mean values of the shape param-
184 eters and Krumbein's chart roundness values are given in column 2 and 3, respec-
tively.

| shape parameters | correlation coefficient | |
|--------------------|--------------------------------|-------------------------|
| | individual values ($n = 81$) | mean values ($n = 9$) |
| b | 0.065 | 0.153 |
| b/a | 0.057 | 0.199 |
| rD | 0.847 | 0.967 |
| rW | 0.919 | 0.992 |
| rP | 0.899 | 0.979 |
| <i>circularity</i> | -0.844 | -0.984 |
| <i>convexity</i> | 0.895 | 0.972 |

Table 1

Correlation between shape parameters values and Krumbein's chart ones (b : size, b/a : elongation, rD : Drevin's roundness, rW : Wadell's roundness, rP : ratio between perimeters of the silhouette and of the best approximating ellipse).

185

186 Our implementation of Wadell's index is the shape parameter that provides the best
187 results with a linear correlation of 92%. This is reassuring since Krumbein (1941)

188 used the method proposed by Wadell (1932) to divide his standard profiles into
189 9 classes having the same roundness value (section 1). Table 1 also shows that
190 the form parameters of *circularity*, *convexity* and rP are also linearly correlated
191 with Krumbein roundness values. However, the correlation coefficients found are
192 lower than the values given in the litterature (section 1). For instance, our imple-
193 mentation of Drevin’s parameter provides a linear correlation of 85% compared to
194 96% in Drevin and Vincent (2002). The discrepancy may be related to differences
195 of implementation (our distance transform is not an approximation but is exact)
196 and of quality of the input image (quality of Krumbein’s chart, acquisition process,
197 resolution, and so on).

198 In figure 8, rW is plotted against the Krumbein roundness classes (rK). The slope
199 of the least square regression line is greater than 2, whereas its y-intercept is around
200 of -0.7, what is far of the straight line of slope 1 and y-intercept 0. Intraclass vari-
201 ance is higher than expected whereas interclass variance is lower than expected. The
202 source of this variance is the lack of corner and curvature definitions in the original
203 paper of Wadell (1932) (section 1). This methodologic gap could also explain the
204 high inter-observer variability of Cailleux roundness index noticed in Pissart et al.
205 (1998).

206 To end this section, we also studied the correlation between each pair of shape pa-
207 rameters and found the following result: there is no correlation between the round-
208 ness parameters rD , rW or rP and elongation or size.

209 **4 Assessment of the longitudinal pattern of particule abrasion**

210 We used our shape parameters in order to study real pebbles from digital images,
211 collected in the bed of the Progo, an Indonesian river located on Java Island near
212 Yogyakarta. The river is 135 km long, has a catchment of 2400 km² and drains sev-
213 eral volcanos, such as the Merapi, still active on the east side (2900 m in elevation)
214 and also the Sumbing and the Sundoro on the west side (3200 m and 3100 m in
215 elevation respectively). The source of the river is on the northern side of Mount
216 Sundoro at 2500 m in elevation (figure 9). 2500 pebbles were randomly sampled in
217 the bed, with 2 to 5 photos being taken on 25 stations located at various distances
218 from the source (in average every 5 km). We analysed an average of 105 pebbles
219 per station (min = 73; max = 154) whose boundary varies between 150 and 620
220 pixels (mean: 330 +/- 70 pixels).

221 In a first step we detected pebbles with clustering methods, transforming the orig-
222 inal color image into a binary image as shown in figure 10. In a second step, we
223 extracted the boundaries from pebbles silhouettes to compute the shape parameters
224 described in section 2. For each sample of pebbles (around 100 pebbles per sam-
225 ple), characterized by its distance from the source, we computed the average value
226 of each shape parameter as well as their confidence level of 0.95, each pebble being
227 picked up randomly.

228 Figure 11 depicts the longitudinal pattern of each parameter along the river course.
229 The different parameters do not show a well structured trend from the mouth to the
230 ocean, which demonstrates the complex origin of the particles located in the main
231 stem. The clearest longitudinal trend was obtained by the convexity ($r^2=0.035$).
232 While each parameter has a unique pattern, rP and *circularity* are highly cor-

233 related (the coefficient of determination r^2 equals -0.928) as are *convexity* and
234 *circularity* ($r^2=-0.899$). rW is the parameter that is the most least correlated with
235 the others. The best correlation is observed for rD ($r^2=0.76$) and the coefficient of
236 determination is less than 0.63 for the three others. A similar general pattern can be
237 nevertheless observed from most of the parameters:

- 238 (1) Angular particles are preferentially observed in the upstream section with
239 a clear trend in roundness development from km 0 to km 20 for rP , rD ,
240 *convexity* and *circularity*, and until km 50 for rW . Therefore, the least
241 round particles are generally observed at the source station (rW , rD , *circularity*,
242 *convexity* and rP parameters).
- 243 (2) For all parameters, a significant decrease in roundness is also observed in the
244 middle of the section (km 60 to km 80).
- 245 (3) Downstream of km 80, all of the parameters exhibit a significant increase
246 in roundness until km 100 but then, they are fairly constant until km 130.
247 With the exception of rW , the roundness estimates are here similar or slightly
248 higher (*convexity* and rP) than those observed between km 25 to km 50.
249 The most rounded particles are observed at the downstream station or close
250 to it (rP , *circularity*, *convexity*). Downstream, rW does not readjust to the
251 disruption that occurs in the middle section and does not reach the highest
252 values until around km 50-55.

253 From a thematic point of view, a nice trend in roundness is observed in the upstream
254 part of the catchment. This trend is clear because no main tributary providing less
255 rounded particles disrupts the abrasion process. The delivery of the Kali Galeh at
256 km 21 is the only perturbation detected by some of the parameters but it does not
257 counteract the trend. It is then possible to fit a law for predicting roundness process
258 in such an andesitic environment using rW ($rW = 0.002 \text{ Km} + 0.69$; $r^2 = 0.87$)

259 or rP parameter ($\text{Log}(rP) = 0.009 \text{ Log}(Km) + 0.69$; $r^2 = 0.90$). These results also
260 underline that such parameters are powerful enough to determine a roundness trend
261 over long distances (e.g. 20 to 50 km) whereas previous works had indicated that
262 roundness only significantly affected particles near the source (the first km) after
263 which it was constant in a downstream direction (Pissart et al. (1998) for exam-
264 ple). The parameters are also robust enough to highlight the major disruption in
265 the roundness trends due to sediment delivery in the middle section from the active
266 Merapi volcano located on the east side. This area is a major source of angular ma-
267 terial that disrupt the longitudinal trend. The distance from the peak of Merapi to
268 the main stem is only 25-30 km. It is then interesting to see that the rW and rD
269 values reached in this section (km 60-80) are then very similar to those observed
270 at km 25-30 of the main stem, which may indicate that the abrasion process on
271 the Merapi slopes is similar to that observed on the Sandoro, which is a much older
272 volcano. The decrease in roundness already occurs by the km 62 and km 67 sta-
273 tions, which is before the confluence with the Kali Elo and Kali Pabelan that drain
274 the Merapi. This indicates that the delivery is not only linked to the river network
275 itself but also from unherited material provided by the Merapi, stored in the allu-
276 vial corridor and delivered by bank erosion. The trends observed downstream the
277 area influenced by the Merapi are more difficult to interpret because the different
278 indicators have contrasting patterns. This raises the possibility of using the differ-
279 ent parameters in combination in order to characterise on a long continuum the
280 abrasion process and the possible substitution of macro-scale to micro-scale shape
281 changes as far as the particle abrades over a few kilometers. In the downstream
282 context of the Progo basin, some parameters, mainly *circularity* and *convexity*,
283 may be more powerful for characterising roundness trend when particle corners are
284 already smoothed. We may then hypothesise that rW would be a better discrimi-
285 nant parameter of roundness upstream in a context of angular particles whereas rP ,

286 *convexity* and *circularity* would be more powerful downstream when the particle
287 corners are already smoothed and the abrasion affects the shape itself.

288 **5 Conclusion and perspectives**

289 These new computer developments are a powerful tool to better understand in field
290 abrasion processes. The automatic imagery procedure allows us to replace the easy-
291 to-collect indices such as Krumbein visual classes and the Cailleux index with the
292 most precise roundness parameter, rW . From this preliminary field analysis, it is
293 clear that the implementation of the rW parameter is useful because it provides a
294 quantification of corner abrasion of particles, which is not entirely the case with
295 the other parameters that are more sensitive to the particle shape than the corner
296 shapes. By providing both corner and shape parameters, the developments allow
297 us to study the abrasion process over a long spatial continuum. We can expect that
298 rW is the most robust in the source context as it is based on all the corners and
299 really describe the corner abrasion, whereas rP , *convexity* or *circularity* provide
300 indications at a macro-scale of abrasion effects on the particle shape. The field ex-
301 ample has been based on average values, but a multivariate analysis is a challenging
302 issue that could better explore the variability of roundness parameters observed at
303 each of the stations and its evolution downstream. It has also been shown that the
304 resolution may affect the quality of the results but that the parameters are fairly ro-
305 bust and allow the comparison of pebbles of various sizes from photos of different
306 resolutions. Threshold values in term of resolution (e.g., number of pixels per peb-
307 ble perimeter) are provided to correctly specify the field collection requirements in
308 term of photo resolution and minimum particle size.

Acknowledgements. The authors want to thank kindly the different colleagues who participate to earlier discussions and debates about characterising pebble roundness and shapes from imagery processing, notably Bernard Lacaze from Prodig, Paris, and Christophe Delacourt from the University of Brest. The experimental sample has been collected in an International Program of Scientific Cooperation led by Franck Lavigne: PICS 1042 “Dynamique sédimentaire et risques naturels dans le bassin du fleuve Progo, Java Centre, Inonésie” (2001-2003).

This work has been partially supported by a grant from the french DGA for Tristan Roussillon.

References

- Abt, S.R., Bunte, K. 2001, Sampling surface and subsurface particle-size distributions in wadable gravel- and cobble-bed streams for analyses of sediment transport, hydraulics, and streambed monitoring. RMRS-GTR-74, USDA Forest Service, Rocky Mountains Research Station, General Technical Report 74.
- Cailleux, A., 1947, L'indice d'émoussé: définition et première application. Comptendu sommaire de la Société géologique de France, 13-14, 251-252.
- Cottet, M. L., 2006, Mesure et structures spatiales et temporelles de l'mouss des galets dans le rseau hydrographique du Bez, Master's thesis, Université Jean Moulin Lyon3, 72 pp.
- Debled-Rennesson, I., Réveillès, J-P., 1995, Linear algorithm for segmentation of digital curves. International Journal of Pattern Recognition and Artificial Intelligence, 9, 635-662.
- Diepenbroek, M., Bartholomä, A., Ibbeken, H., 1992, How round is round? A new approach to the topic 'roundness' by Fourier grain shape analysis. Sedimentol-

- ogy, 39, 411-422.
- Drevin, G.R., Vincent, L., 2002, Granulometric determination of sedimentary rock particle roundness, in International Symposium on Mathematical Morphology, 315-325.
- Hirata, T., 1996, A unified linear-time algorithm for computing distance maps. Information Processing Letters, 58, 3, 129-133.
- Klette, R., Zunic, J., Multigrid Convergence of Calculated Features in Image Analysis, Journal of Mathematical Imaging and Vision 13, 173-191, 2000
- Krumbein, W.C., 1941, Measurement and geological significance of shape and roundness of sedimentary particles. Journal of Sedimentary Petrology, 11, 2, 64-72.
- Melkman, A.A., 1987, On-line construction of the convex hull of simple polygon. Information Processing Letters, 25, 11, 11-12.
- Nguyen, T.P., Debled-Rennesson, I., 2007, Curvature Estimation in Noisy Curves. 12th International Conference on Computer Analysis of Images and Patterns, Vienna, (August 2007).
- Pissart, A., Duchesne, F., Vanbrabant, C., 1998, La détermination pratique des intervalles de confiance des comptages de cailloux et des mesures d'éroulé. Comparaison des mesures d'éroulé de Cailloux et de Krumbein. Géomorphologie: relief, processus, environnement, 3, 195-214.
- Preparata, F.P., Shamos, M.I., 1985, Computational geometry: an introduction. Springer.
- Toussaint, G.T. Solving geometric problems with the rotating calipers, Proc. MELECON '83, Athens (May 1983).
- Wadell, H., 1932, Volume, shape, and roundness of rock particles. Journal of Geology, 40, 443-451.

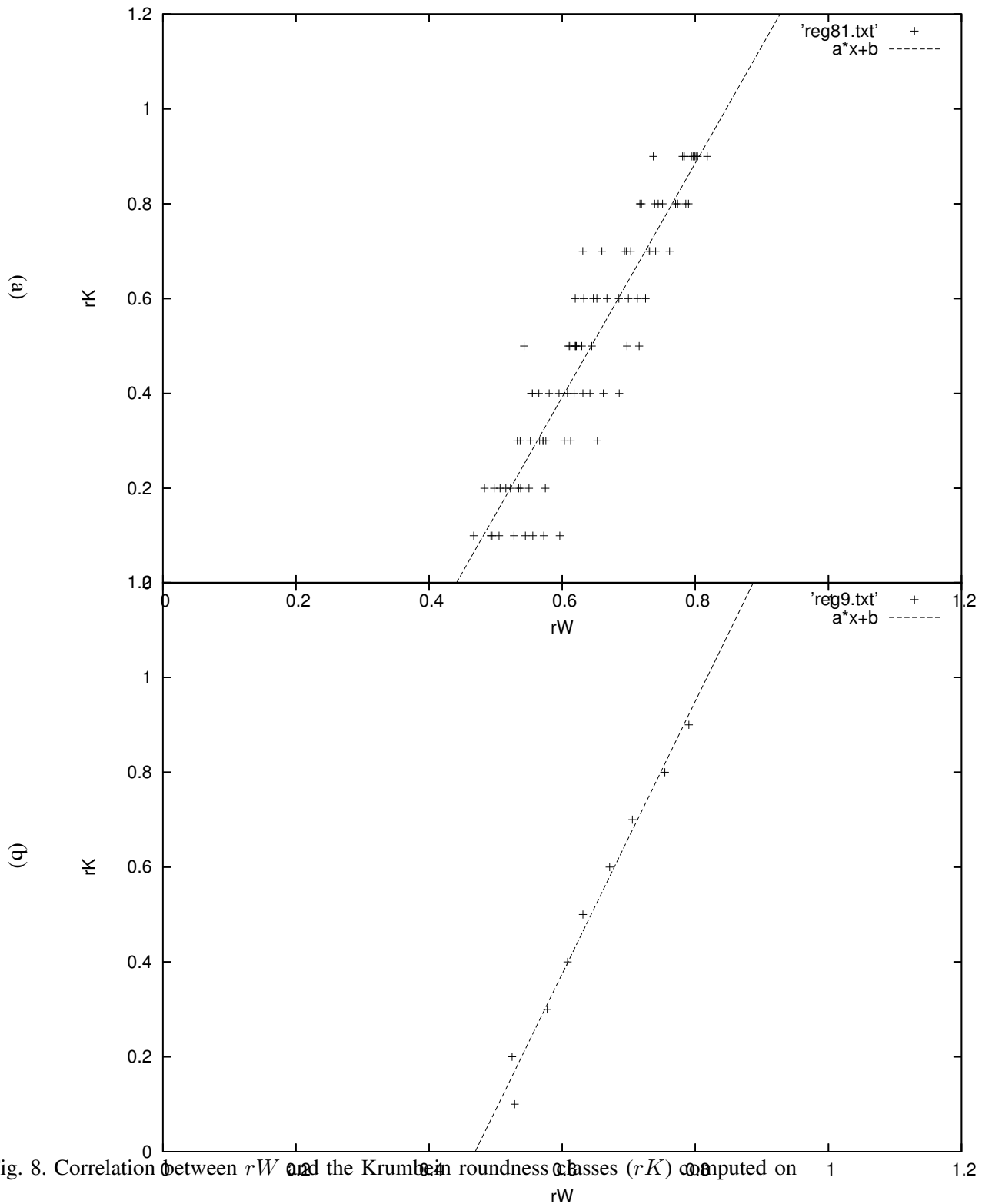


Fig. 8. Correlation between rW and the Krumbein roundness classes (rK) computed on individual values in (a) (each crosses depict a silhouette of Krumbein's chart) and on mean values in (b) (the nine cross depicts the nine roundness classes of Krumbein's chart).

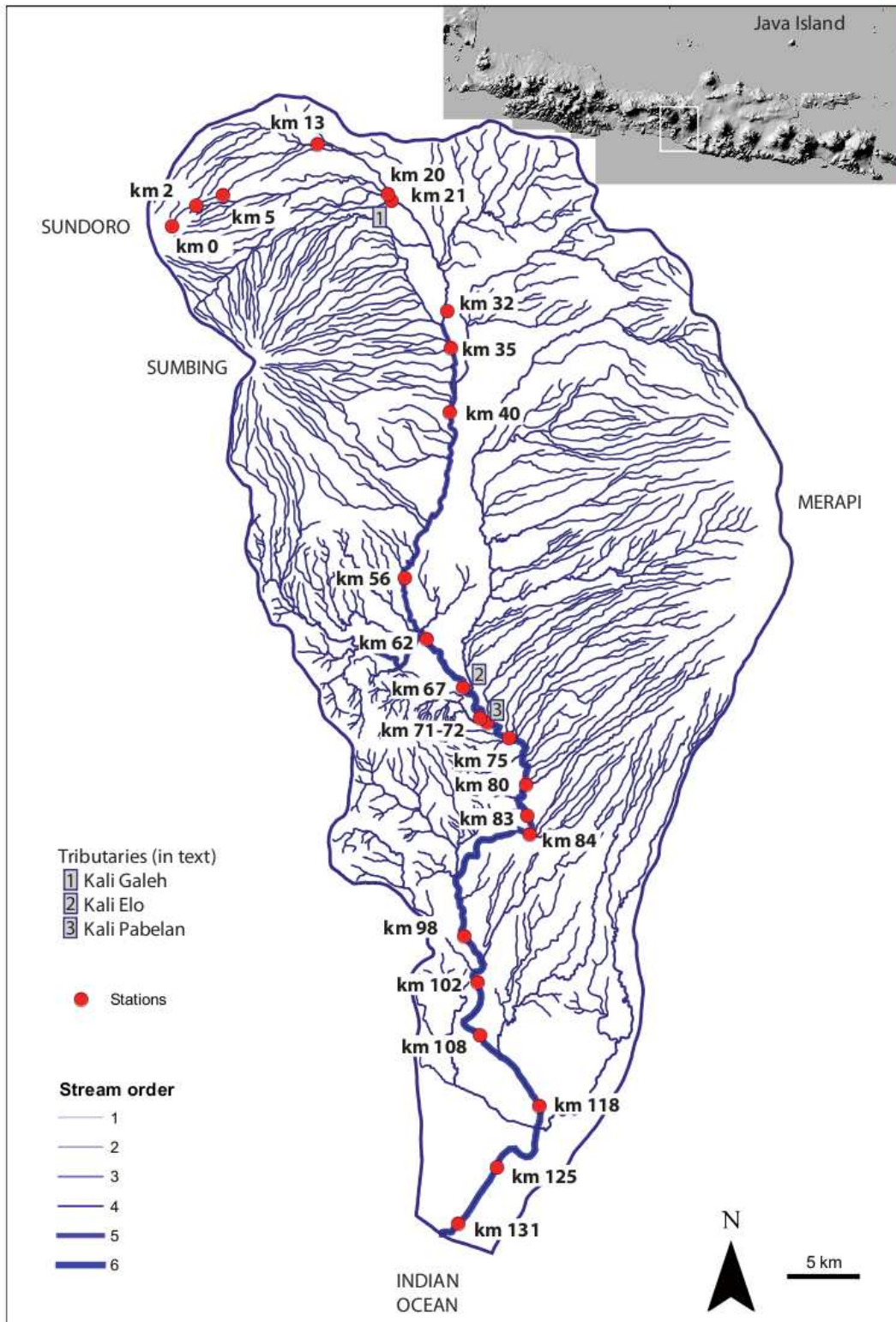
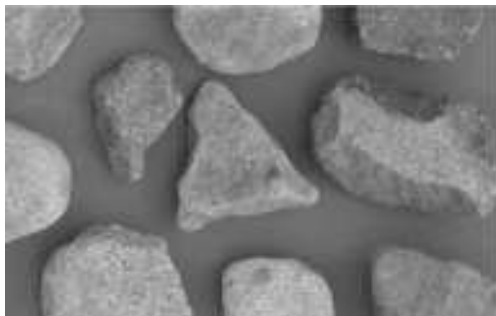


Fig. 9. The catchment of the Progo River, Java island, Indonesia. Note the structure of the hydrographic network that is strongly controlled by the volcanoes. The 25 stations are located along the main stem from the Sundoro volcano to the Indian Ocean and their distances to the source (in km) are indicated.



(a)



(b)



(c)

Fig. 10. A image of sample pebbles with boundaries extracted in white (a). The extraction is performed by contour tracking in the binary image (b). The last is computed with clustering methods applied to the original color image (c).

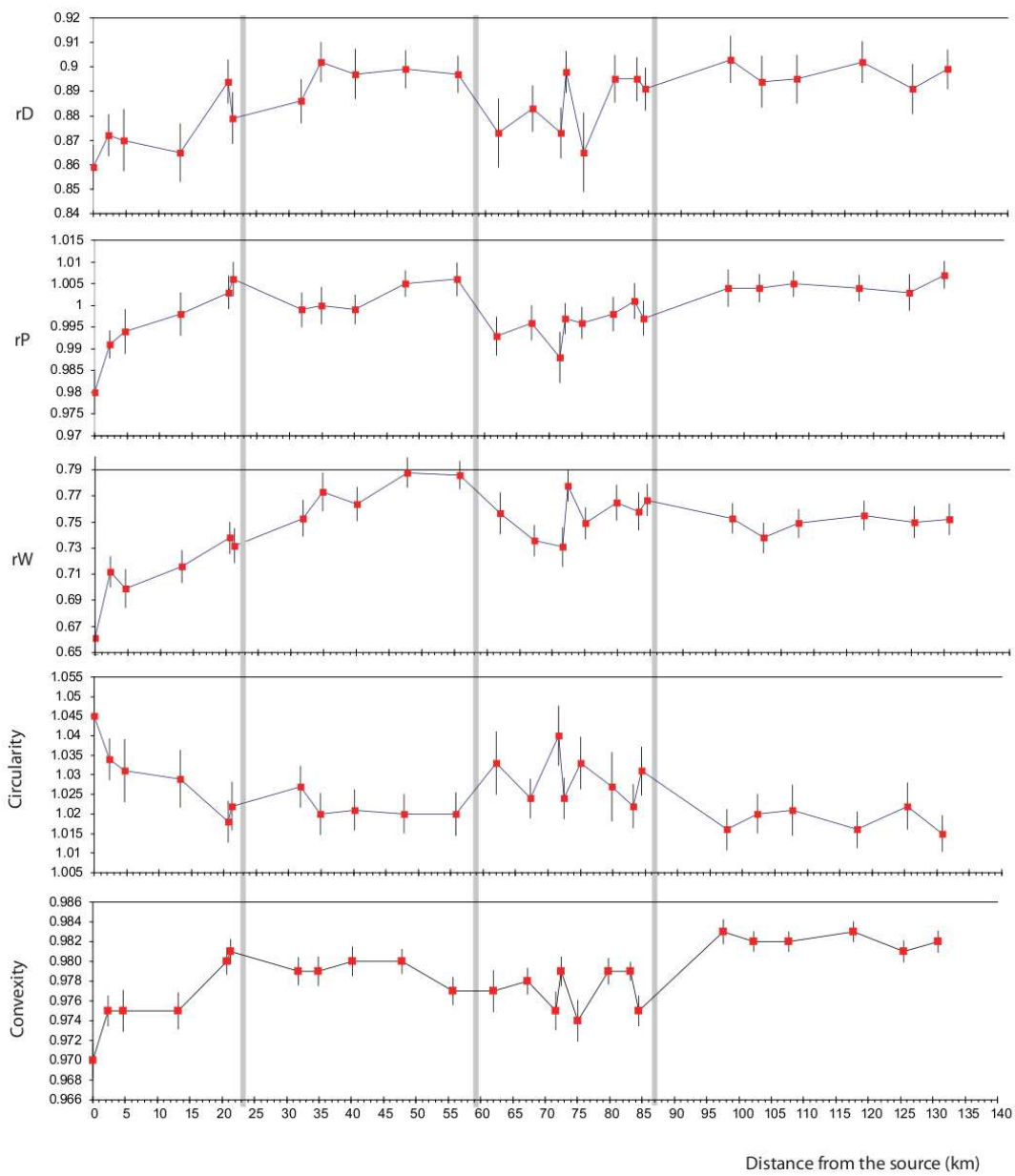


Fig. 11. Longitudinal pattern of our implementation of Wadell's method (rW), Drevin's method (rD), perimeter ratio (rP), circularity and convexity from the source of the Progo (km 0) to the ocean (km 130).